Charge Separation is Virtually Irreversible in Photosystem II Core Complexes with Oxidized Primary Quinone Acceptor

ARTICLE *in* THE JOURNAL OF PHYSICAL CHEMISTRY A · FEBRUARY 2011

Impact Factor: 2.69 · DOI: 10.1021/jp1083746 · Source: PubMed

4 AUTHORS, INCLUDING:

Jan P Dekker
VU University Amsterdam
175 PUBLICATIONS **8,821** CITATIONS
SEE PROFILE

Rienk van Grondelle
VU University Amsterdam
647 PUBLICATIONS **23,660** CITATIONS
SEE PROFILE

Ivo H M Van Stokkum
VU University Amsterdam
280 PUBLICATIONS **10,114** CITATIONS
SEE PROFILE

THE JOURNAL OF PHYSICAL CHEMISTRY A

ARTICLE

pubs.acs.org/JPCA

Charge Separation is Virtually Irreversible in Photosystem II Core Complexes with Oxidized Primary Quinone Acceptor

C. D. van der Weij−de Wit, J. P. Dekker, R. van Grondelle,* and I. H. M. van Stokkum

Department of Physics and Astronomy, Faculty of Sciences, VU University Amsterdam, De Boelelaan 1081, 1081 HV Amsterdam, The Netherlands

Supporting Information

ABSTRACT: X-ray structures of the Photosystem II (PSII) core revealed relatively large interpigment distances between the CP43 and CP47 antenna complexes and the reaction center (RC) with respect to the interpigment distances in a single unit. This finding questions the possibility of fast energy equilibration among the antenna and the RC, which has been the basic explanation for the measured PSII fluorescence kinetics for more than two decades. In this study, we present time-resolved fluorescence measurements obtained with a streak-camera setup on PSII core complexes from *Thermosynechococcus elongatus* at room temperature (RT) and at 77 K. Kinetic modeling of the RT data obtained with oxidized quinone acceptor Q_A, reveals that the kinetics are best described by fast primary charge separation at a time scale of 1.5 ps and slow energy transfer from the antenna into the RC, which results in an energy equilibration time between the antenna and the RC of about 44 ps. This model is consistent with structure-based computations. Primary radical pair formation was found to be a virtually irreversible process. Energy equilibration within the CP43 and CP47 complexes is shown to occur at a time scale of 8 ps. Kinetic modeling of the 77 K data reveals similar energy transfer time scales in the antenna units and among the antenna and the RC as at RT, respectively, 7 and 37 ps. We conclude that the energy transfer from the CP43/CP47 antenna to the RC is the dominant factor in the total charge separation kinetics in intact PSII cores.

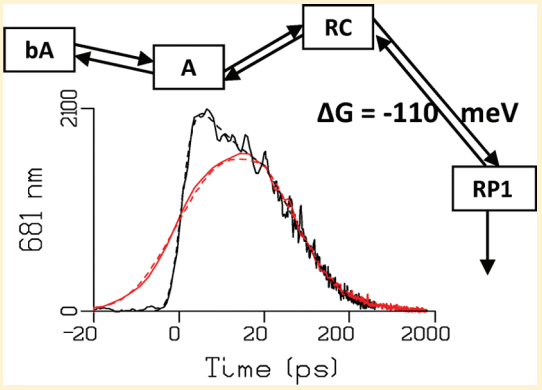

INTRODUCTION

Photosystem II (PSII) is a large supramolecular pigment−protein complex that is embedded in the thylakoid membrane of plants, cyanobacteria, and algae. In oxygenic photosynthesis, PSII catalyzes water splitting to create a proton gradient across the membrane and to form oxygen, using light energy as the driving force. PSII consists of a core complex surrounded by several antenna pigment−protein complexes, which efficiently collect light and transfer the energy into the core.[1] The X-ray structure of the cyanobacterial PSII core has been resolved up to 2.9 Å resolution.[2−5] Natively, PSII cores are organized into dimers in the stacked parts of the membrane.[6] The PSII core consists of at least 17 subunits.[5] Proteins PsbB and PsbC bind respectively 16 and 13 Chl *a* and are known as the CP47 and CP43 core antenna complexes, which flank both sides of the PSII reaction center (RC), comprised respectively by PsbA and PsbD. CP43 and CP47 take care of the efficient transfer of light energy into the RC. In the RC, light energy is used for charge separation (CS), resulting in the water splitting. PsbA and PsbD provide the ligands for the cofactors present in the electron transfer chain, where PsbA constitutes the active branch and PsbD the inactive branch.[7] The cofactors are 6 Chl *a*, 2 Pheo *a*, 2 plastoquinones (Q_A, Q_B), 2 redox-active tyrosines (Y_Z, Y_D), a nonheme iron, and the manganese cluster. Upon excitation of the RC at least two possible pathways for charge separation exist.[8−10] The major fraction induces electron transfer from Chl_{D1} to Pheo,[11−13] a minor fraction starts from the special pair $P_{D1}P_{D2}$.[9] The final product for both pathways is $P_{D1}^{+}Pheo_{D1}^{-}$, from where the electron is passed through to the quinone acceptor Q_A (for reviews on charge separation, see refs 7, 14, and 15). P_{D1}^{+} subsequently withdraws an electron from the manganese cluster, mediated by Y_Z. Upon the uptake of four photons resulting in CS, Q_A doubly reduces two mobile Q_B molecules, whereas at the manganese cluster the four positive charges possess enough strength to oxidize two water molecules. Four hydrogen ions associate with the two doubly reduced Q_B molecules. The H_2Q_B complexes are released into the plastoquinone pool and are replaced by a Q_B from the pool.

Early time-resolved studies on PSII cores revealed the excitation energy trapping to be multiphasic.[16−18] The Exciton Radical Pair Equilibrium (ERPE) model was developed to describe this behavior.[19,20] In this model, the RC forms a shallow trap from which reversible CS is possible. The main assumption of the model is the occurrence of fast energy equilibration over the core antenna and RC prior to CS. As a result, the model describes trap-limited CS in the PSII cores. The trapping time scales were found to depend on the presence of antenna units as well as the

Special Issue: Graham R. Fleming Festschrift

Received: September 2, 2010
Revised: January 7, 2011

   dx.doi.org/10.1021/jp1083746 | *J. Phys. Chem. A* XXXX, XXX, 000–000

redox state of the primary quinone acceptor Q_A.[19,21] Nowadays, the time scale of the energy equilibration over the complex is under debate,[15] because from the X-ray structure[5] the interpigment distance between antenna and RC (∼20 Å) appears rather large with respect to the interpigment distance within a single unit (5−10 Å), which may limit energy transfer to the RC.[15,22−27]

Miloslavina et al.[28] measured the fluorescence kinetics of intact PSII cores with open RCs, using the single photon counting technique. They were the first ones to resolve emission decay components on the short time scale, namely, 2 and 9 ps. The 2 ps decay was assigned to fast excitation energy transfer from the antenna into the RC and the 9 ps component was split into 7 and 10 ps contributions by, respectively, primary radical pair (RP1) formation and energy equilibration between CP43 to CP47 through the RC. The commonly known ∼40 ps main excitation energy trapping component of the PSII core was assigned to second radical pair (RP2; P^+Pheo^-) formation. In their modeling, Miloslavina et al.[28] thus assume the energy transfer among the core antenna and the RC to be unreasonably fast with respect to the predictions from the molecular structure, as discussed in ref 15. Also, Broess et al.[29] suggest a very fast energy transfer. In contrast, Pawlowicz et al.[27] show in their femtosecond mid-infrared spectroscopic study of the PSII core that slow energy transfer from the CP43 and CP47 antennae to the RC is the physical origin of the 40 ps main excitation energy trapping component in PSII cores.

The lack of consensus on the interpretation of time-resolved studies of the PSII core calls for new measurements and analysis. In this study we aim to enlighten the role of excitation energy transfer from the antenna into the RC in the total CS process for PSII cores with open, functional reaction centers. We employ a streak camera[30−32] system with high time resolution. To this end, room temperature time-resolved fluorescence was measured of PSII cores from *Thermosynechococcus elongatus* with Q_A oxidized, with a setup that offers the possibility to simultaneously measure the fluorescence decay over a ∼300 nm wavelength range with far better time-resolution (typically 5 ps fwhm) than the single photon counting detection technique used by Miloslavina et al.[28] (typically 30 ps fwhm). The measurements were also performed at 77 K to obtain more details on the transfer of excitation energy from the core antenna to the RC.

MATERIALS AND METHODS

Sample Preparation. Dimeric PSII core complexes with both Q_A and Q_B present were isolated from *Thermosynechococcus elongatus* and purified as described in ref 33. In brief, after cell disruption and centrifugation, thylakoid membranes were solubilized with n-ss-D-dodecylmaltoside (ss-DM) and PSII was purified using a two-step anion exchange chromatography. The dimeric PSII was further purified by crystallization using PEG 2000 as precipitant. The obtained microcrystals were redissolved in 100 mM Pipes-NaOH, 5 mM $CaCl_2$, and 0.03% ss-DM. The concentrated protein solution was frozen in liquid nitrogen and stored at 77 K. The PSII complexes are characterized by an O_2 flash yield of about 6×10^{-3} O_2/Chl per flash.

Time-Resolved Emission. Briefly, 400 nm, vertically polarized excitation pulses of 100−200 fs were generated using the frequency doubled output of a Ti:sapphire laser (Vitesse, Coherent St. Clara, CA) and a regenerative amplifier (REGA, Coherent). Fluorescence light was collected at right angle to the excitation light, under magic angle through an orange sharp cut off filter, using a Chromex 250IS spectrograph and a Hamamatsu C 5680 synchroscan streak camera. The streak images were recorded with a cooled, Hamamatsu C4880 CCD camera.

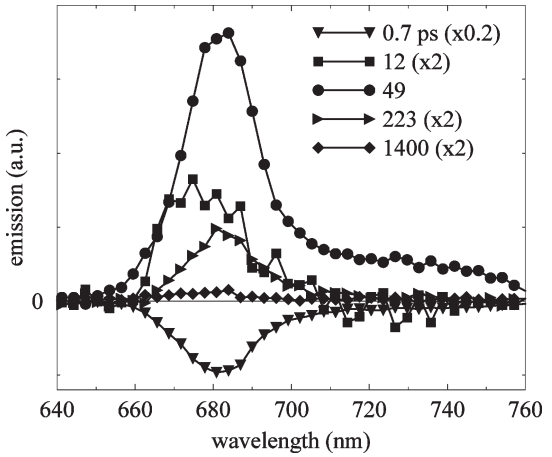

Figure 1. DAS of intact PSII cores with open RCs at room temperature upon 400 nm excitation.

For the room temperature measurements, the excitation light was collimated with a 15 cm focal length lens, resulting in a focal diameter of 150 μm in the sample. The laser repetition rate was 300 kHz and the pulse energy 0.1 nJ. The sample was in a 2 mm spinning cell of 10 cm diameter, rotating at a frequency of 75 Hz. PSII cores were diluted to an optical density of 0.6 cm^{-1} at 673 nm in a buffer of 20 mM MES pH 6.5, 10 mM $CaCl_2$, 10 mM $MgCl_2$, 400 mM mannitol, 0.06% β-DM, and 5 mM ferricyanide was added to keep Q_A oxidized. Under these low excitation density conditions (∼1 absorbed photon per 50 dimeric cores), the experiments are expected to be free of annihilation.

For the 77 K measurements, an unfocused excitation beam was used with a diameter of ∼1 mm. The laser repetition rate was 50 kHz and the pulse energy was 10 nJ. The sample was in a 1 cm polystyrene cuvette in a nitrogen cryostat (Oxford). At 77 K, the fluorescence was detected in front-face mode. PSII cores were diluted in a buffer of 65% v/v glycerol, 20 mM MES pH 6.5, 10 mM $CaCl_2$, 10 mM $MgCl_2$, 400 mM mannitol, and 0.09% β-DM to an optical density of 1.0 cm^{-1} at 673 nm.

The fluorescence was measured on time bases of 500 and 2000 ps, with respective full-width at half-maximum (fwhm) of the overall time response of 5 and 21 ps at room temperature and 9 and 21 ps at 77 K. In the global analysis, both the instrument response and time dispersion were free parameters of the fit.

The data sets obtained with the streak camera setup, consist of two-dimensional images of fluorescence intensity as a function of both time and wavelength. Before analysis, the images are corrected for background and sensitivity of the detection system. The images are sliced up into time traces which span 4 nm. In global analysis, the time traces are fit with a sum of exponentials with different decay times. The amplitudes of these exponentials as a function of emission wavelength result in so-called decay associated spectra (DAS). In these spectra, positive amplitude represents a loss of fluorescence, whereas negative amplitude reflects a rise of fluorescence. A DAS with positive amplitude at short wavelengths and negative amplitude at higher wavelengths thus represents an energy transfer process, whereas an overall positive spectrum describes either trapping of excitations by CS or a natural fluorescence emission of the pigments (the latter occurs typically on the nanosecond time scale). In target analysis, a kinetic model consisting of several pigment pools

dx.doi.org/10.1021/jp1083746 |J. Phys. Chem. A XXXX, XXX, 000–000

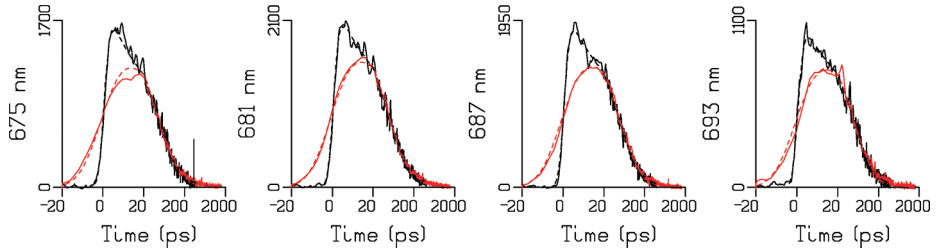

Figure 2. Fluorescence time traces (solid) and the global fit (dash) of Figure 1 on a time scale of 0.5 ns (black) and 2 ns (red), with respective instrument responses of 5 and 21 ps fwhm, for wavelengths 675, 681, 687, and 693 nm. Note that the time axis is linear from −20 to 20 ps and logarithmic thereafter.

interconnected by energy/electron transfer rate constants is fit to the data, resulting in species associated spectra (SAS). For details, see the Supporting Information and refs 31, 34, and 35.

RESULTS AND DISCUSSION

Room Temperature Time-Resolved Emission. Time-resolved fluorescence was recorded at room temperature upon 400 nm excitation. The initial excitation population will thus be homogeneously distributed over all chlorophylls and pheophytins of the PSII core complex. The fluorescence time traces were subjected to global analysis. The estimated DAS are shown in Figure 1. The data could be well described by 5 decay components. The first resolved DAS with a decay time of 0.7 ps shows overall negative amplitude with maximum at 681.5 nm and is assigned to the fluorescence rise due to Soret to Q_y relaxation. For details, see the Supporting Information. The second DAS is associated with a 12 ps decay time and is multiplied in Figure 1 by a factor of 2 for clarity. This DAS has a positive maximum between 669 and 687 nm. The main (well-known) PSII core decay component was resolved to have a 49 ps lifetime, with emission maximum at 682 nm. The fourth DAS has only minor amplitude, a 223 ps time constant and a maximum emission at 682 nm, which is multiplied in Figure 1 by a factor of 2 for clarity. Careful analysis revealed a 1.4 ns lifetime component, which is estimated to trap less than 1.5% of the initial excitations and has a noisy spectrum. Both the 49 and 223 ps decay times are values commonly found in the literature on PSII cores with Q_A oxidized.[21,24,28] However, in our data, the fluorescence decay on the ns time scale was almost negligible, in contrast with other studies on PSII cores where the PSII RC was claimed to be open.[21,24]

Figure 2 displays a selection of time traces with their fits (the concomitant residuals are depicted in Figure SI.1) showing both the fit quality and the near absence of long lifetime fluorescence, because there is hardly emission left after 1 ns. It is known that it is really hard to avoid closure of a small fraction of PSII RCs, which results in the presence of ns decay components. In fact, it took us multiple efforts, varying excitation density, data acquisition time per PSII core sample, and electron acceptor concentration before we managed to get to the right set of conditions in which >98.5% of the RCs remain open. The main problem was to tune the time it takes for a sample volume to get re-excited and the Q_A^- oxidation time by the electron acceptor, such as to avoid re-excitation of the small fraction of PSII cores with reduced Q_A. As a result, one should either have a big reservoir of PSII cores or one can measure with really low excitation density for only a short period on a limited amount of sample (at the cost of the signal-to-noise (S/N) ratio) to be sure not to re-excite unrelaxed cores. However, in all our different efforts, the

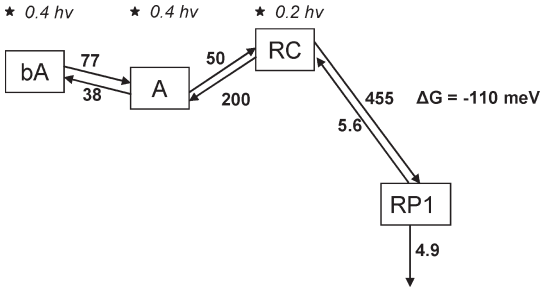

Figure 3. Kinetic model to describe the results of Figure 1. The compartment bA represents the blue absorbing Chls in the CP43/CP47 antenna, which are in equilibrium with the bulk Chls of the antenna (A). The excited RC Chls are represented by (RC), which are in equilibrium with both the core antenna and the first radical pair (RP1). ★ indicates the initial excitation fractions: 40% bA, 40% A, and 20% RC. Rate constants (ns^{-1}) estimated are indicated in the figure as well as the RC-RP1 free energy. Resulting lifetimes: 1.5, 7.7, 44, and 225 ps. The estimated error in the lifetimes is 10%.

~10 ps decay with the characteristic contribution of blue 670−675 nm emission (Figure 1) was present (not shown). We emphasize that our 12 ps DAS differs significantly from the 9 ps DAS resolved by ref 28, which has its emission maximum at 685 nm: the 12 ps DAS in Figure 1 has extra amplitude of similar size around 673 nm. The blue (673 nm) emission amplitude in the 12 ps DAS with respect to those with 49 and 223 ps decay time (682 nm maximum) demonstrates the occurrence of energy transfer from blue to more red absorbing Chls *a* on this time scale. The absence of negative amplitude at wavelengths above 673 nm in the 12 ps DAS indicates the simultaneous decay of the emission at these more red wavelengths at the same, or a faster, time scale due to trapping.

Kinetic Modeling. To unravel the processes underlying the spectral evolution taking place on the different time scales estimated in global analysis, a target analysis was performed. In target analysis, a kinetic model is established, which satisfactorily describes the fluorescence decay. The minimal model, which successfully describes the recorded room temperature PSII core kinetics, comprises four compartments and is shown in Figure 3 with the optimal rate constants and free energy associated with RP1 formation. Further explanation can be found in the Supporting Information. The S/N quality of the data and the small difference in spectral characteristics of CP47 and CP43 at room temperature did not allow CP43 and CP47 to be spectrally distinguished. Therefore, we considered CP43 and CP47 as a single entity, the antenna. The model, however, takes into account the presence of a fraction of pigments that absorb more to the blue than the other pigments in the CP43/CP47 antenna.[36] This distinction is made by describing these respective pigment

dx.doi.org/10.1021/jp1083746 |J. Phys. Chem. A XXXX, XXX, 000–000

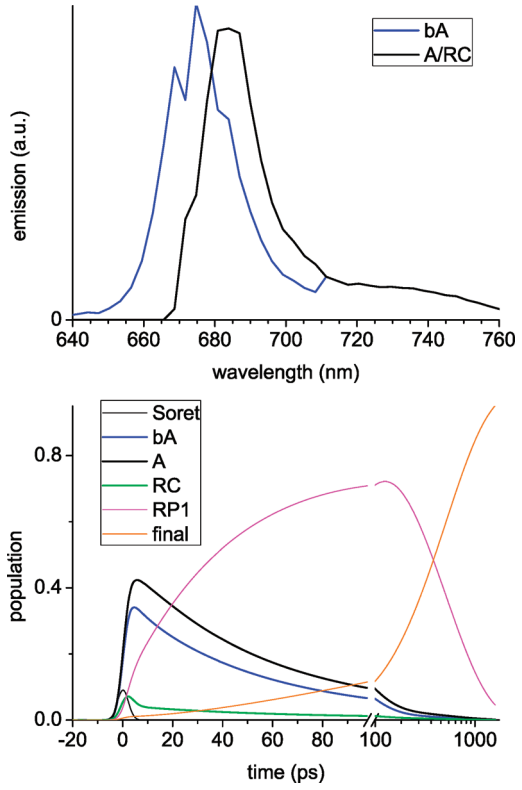

Figure 4. (top) Estimated SAS from the model given in Figure 3. Key: bA (blue); A and RC (black), which have been assumed to have equal spectra. RP1 is nonfluorescent, (bottom) population profiles of all species.

pools with the two compartments (bA) and (A) in the model of Figure 3, where (bA) equilibrates with (A). Then, we can describe the fluorescence kinetics well by further equilibration of the relaxed antenna (A) with the RC (RC). From the RC CS can occur formation of (RP1), which is reversible, as shown by the back transfer, whereas from RP1 the excitation energy is irreversibly trapped by the 4.9 ns^{-1} process. In reality, electron transfer in the RC comprises multiple steps before Q_A^- becomes oxidized by ferricyanide, implying that, in the model of Figure 3, the single rate for charge separation must be viewed as an "effective" rate.[9,11,12,14] In this study, the minimal model to describe the recorded fluorescence kinetics takes only two CS phases into account. We will come back to this point later.

To control the model within the limits of data quality, we assumed that the emission spectrum of the relaxed antenna (A) is (more or less) equal to that of the RC (RC). The high spectral overlap of the room temperature emission spectra of CP43, CP47, and RC[37] supports the plausibility of this assumption. Spectral constraints are useful in that they facilitate greater insight into the system under study, in particular, the rate constants, as the number of free parameters is reduced. Figure 4 (top) displays the SAS estimated from the modeling of Figure 3, and in the bottom, the populations of the species are depicted. The blue antenna (bA) shows an emission maximum at 675 nm, whereas the relaxed antenna (A) and the RC (RC) have their emission peak at 684 nm. RP1 does not fluoresce. The initial excitation ratio between bA, A, and RC was estimated to be 40:40:20. This ratio is in accordance with the near 20% contribution of the RC to the total amount of Chls *a* in the PSII core and the additional absorption by the two Pheos in the RC at 400 nm. Similarly, from

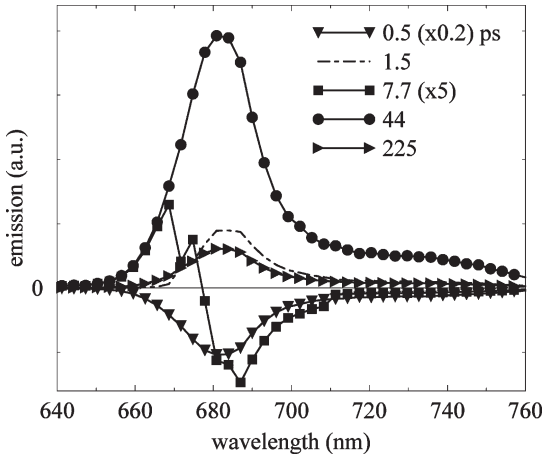

Figure 5. DAS calculated with the help of the kinetic model of Figure 3. See Table 1 for the associated amplitude matrix of the different compartments used in the model.

Table 1. Amplitude-Matrix for the Target Analysis of the Time-Resolved Fluorescence of Intact PSII Cores with Open RCs at Room Temperature, as Presented in Figures 3−5[a]

	bA	A	RC	RP1
τ (ps)	0.4 hν	0.4 hν	0.2 hν	
1.5	0.006	−0.081	0.182	−0.142
7.7	0.056	−0.071	−0.015	0.026
44	0.304	0.479	0.018	−0.975
225	0.034	0.073	0.015	1.091

[a] Negative amplitude represents a population rise, whereas positive amplitude shows population decay of the respective compartment with the specified lifetime.

the rate constants in Figure 3, it is observed that the equilibrium between the RC and the antenna is for more than 80% at the side of the antenna ($k_{RC\text{-}A} = 4k_{A\text{-}RC}$). The lifetimes estimated in the target analysis are 0.5, 1.5, 7.7, 44, and 225 ps. Due to the spectral constraints imposed in the target analysis it became possible to resolve the additional 1.5 ps decay time with respect to global analysis (Figure 1). The longer lifetimes are in good accordance with those estimated in the global analysis.

Because each estimated fluorescence lifetime is a function of all the decay rates present in the system, each compartment will have some contribution at the different lifetimes. From the target analysis of Figure 3, DAS can be calculated and are shown in Figure 5. For details on this calculation, see the Supporting Information. The amplitude matrix is presented in Table 1. We will focus on the main lifetime contributions for each compartment. On the subps time scale, bA, A, and RC become populated from the Soret in the ratio 40:40:20. The lifetime of 1.5 ps is observed (Figure 5) to describe fluorescence decay with emission maximum at 684 nm. From Table 1 it is seen that this lifetime represents trapping of excitation energy from the RC by primary CS, that is, formation of RP1, upon direct excitation of the RC. From the model in Figure 3, RP1 is observed to form a deep trap, with free energy difference with the RC of −110 meV and a very minor back transfer rate. The DAS of the 7.7 ps lifetime is observed to describe energy transfer from pigments emitting at 670 nm (positive amplitude) to those emitting at 684 nm (negative amplitude; Figure 5). The amplitude matrix (Table 1) reveals that

dx.doi.org/10.1021/jp1083746 |*J. Phys. Chem. A* XXXX, XXX, 000–000

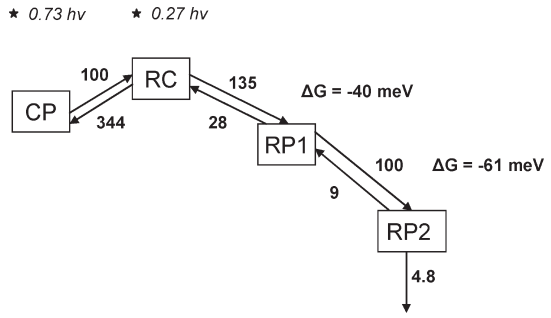

Figure 6. Kinetic model to describe the results of Figure 1, conform.[28] The compartment CP represents the total core antenna. The excited RC (RC) is in equilibrium with both the core antenna and the first radical pair (RP1). RP1 is in equilibrium with the second radical pair (RP2), which irreversibly traps the excitation energy. ★ indicates the initial excitation fractions: 73% CP and 27% RC. Rate constants (ns^{-1}) estimated are indicated in the figure as well as the RC-RP1 and RP1-RP2 free energy. Resulting lifetimes: 1.8, 7, 46, and 249 ps. The estimated error in the lifetimes is 10%.

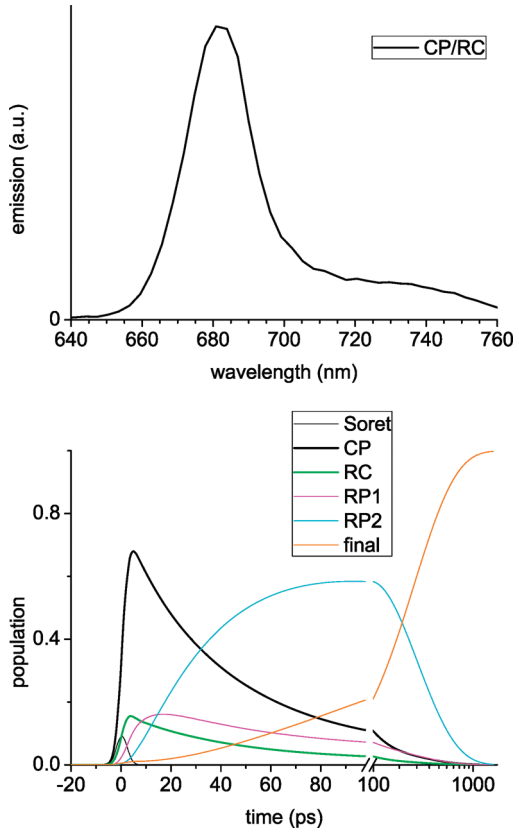

Figure 7. (Top) Estimated SAS from the model given in Figure 6, describing the assumed spectral equality of CP43/CP47 antenna and RC with emission maximum at 682 nm. RPs are nonfluorescent. (Bottom) Population profiles of all species.

this transfer belongs to the excitation energy equilibration between bA and A pigments in the CP43/CP47 antenna. It is unclear, why this equilibration time is about twice as large as was estimated earlier (at 77 K) in isolated CP43 and CP47.[38] As an aside, note that also within the RC slow equilibration with blue absorbing chlorines is present.[9,13,39] The DAS with 44 ps lifetime and emission maximum at 682 nm (Figure 5) has a significantly

Table 2. Amplitude-Matrix for the Target Analysis of the Time-Resolved Fluorescence of Intact PSII Cores with Open RCs at Room Temperature, as Represented in Figures 6 and 7[a]

	CP	RC	RP1	RP2
τ (ps)	0.73 hν	0.27 hν		
1.8	−0.08	0.10	−0.03	0.006
7.5	0.04	−0.004	−0.17	0.164
46	0.68	0.15	0.1	−1.17
249	0.09	0.024	0.1	1.00

[a] Negative amplitude represents a population rise, whereas positive amplitude shows population decay of the respective compartment with the specified lifetime.

larger amplitude and is 2 nm blue-shifted with respect to the 1.5 ps DAS, which is indicative of a role of the antenna in this slow decay phase. From Table 1 it is clearly observed that this lifetime is associated with primary CS and that the energy comes dominantly from bA and A, as judged from their significant positive amplitudes at this lifetime. Thus, RP1 formation on the 44 ps time scale arises due to slow energy transfer from the CP43/CP47 antenna to the RC, whereas CS from the directly excited RC occurs on a very fast time scale of 1.5 ps (Table 1). The decay amplitude of the excited RC is small for the 44 ps lifetime (Table 1) because of the inverted kinetics taking place: the excited state of RC becomes populated on a slower time scale (44 ps), then it decays into RP1 (1.5 ps). Therefore, the RC population remains small (green in Figure 4, bottom). Finally, RP1 is observed to decay with a 225 ps lifetime (Table 1). If we compare the estimated time scales in this study of RP1 formation (1.5 and 44 ps) and trapping (225 ps) with former studies, RP1 can likely be assigned to a mixture of $Chl_{D1}^{+}Pheo^{-}$, $P_{D1}^{+}Chl_{D1}^{-}$, and $P_{D1}^{+}Pheo^{-}$,[9] whereas the trap will be formed by the $P_{D1}^{+}Q_A^{-}$ radical pair.[14]

Important observations from these room temperature data analyses are that (1) the excitation energy equilibration within the CP43/CP47 antenna (bA ↔ A) takes place on a slower time scale (7.7 ps) than assumed in the ERPE model (<3 ps);[19] (2) this is even more dramatically true for the excitation energy equilibration between the CP43/CP47 antenna and the RC, which effectively occurs on a 44 ps time scale; and (3) CS from directly excited RC occurs on the very fast time scale of 1.5 ps and is nearly irreversible. We can thus conclude from this analysis that excitation energy trapping in intact PSII cores with Q_A oxidized can be described well by a model characterized by slow transfer from the antenna to the trap and a fast CS reaction.

Other Kinetic Models. To compare our conclusions with the results of Miloslavina et al.[28] on PSII core kinetics with open RCs, we tried to fit their proposed kinetic model to our data, see Figures 6 and 7 for the model and its SAS, respectively. These authors concluded from their modeling that the energy transfer between core antenna and RC is much faster than CS, in contrast with our model described above. The quality of the fit of the model of Miloslavina et al.[28] is equal to that of the model displayed in Figure 3 (results not shown) and, thus, indicates that neither model is a unique way to describe the data. In this fit (Figure 6), lifetimes of 1.8, 7.5, 46, and 249 ps are estimated, which are highly similar to the values found by Miloslavina et al.[28] (1.5, 7, 10, 42, and 351 ps). We note, however, that they required two more components with lifetimes of 111 and 2350 ps that were not assigned to a physical process. The 10 ps lifetime, absent

dx.doi.org/10.1021/jp1083746 |J. Phys. Chem. A XXXX, XXX, 000–000

in our fit, was assigned to the equilibration between CP43 and CP47 through the RC. Because we do not spectrally discern between the two antenna units (because the spectral differences are too small to allow such a distinction), we cannot verify the presence of this component in our data. Table 2 displays the amplitude matrix associated with the model in Figure 6, from which it can be seen that energy equilibration between the RC and CP43/CP47 antenna according to this model occurs on the 1.8 ps time scale; RP1 formation takes place with a 7.5 ps time constant; dominant population decay of the CP43/CP47 antenna, the RC and RP1 occurs on the time scale of 46 ps and finally the energy becomes trapped from RP2 at the time scale of 249 ps. A larger drop in free energy is found for the RP1 to RP2 (61 meV) transition, with respect to the primary−RC to RP1−CS (40 meV; Table 2). All these observations are highly similar to the findings by Miloslavina et al.[28]

We conclude that both our model (Figure 3) and that proposed by Miloslavina et al.[28] (Figure 6) describe the actual fluorescence data equally well. In both cases, the spectral degeneracy of the CP43, CP47, and RC complexes and their respective pigment contents causes the excited state equilibrium to be at the side of the antenna. Due to this equilibrium, the *apparent* excited state decay time of the antenna will be longer than the *intrinsic* energy transfer time from the antenna into the RC. Another reason for the deviation between these two time scales is the amount of back transfer occurring from the RPs to the RC excited state, as well as the rate of CS. These rates cause the excitations to travel back and forth between the RPs and the antenna, resulting in an increased time spent in the antenna, due to the A-RC equilibrium. In Miloslavina's model, RP1 formation occurs on a time scale of 7.5 ps and the back transfer into the RC is rather significant. Therefore, the RC population is relatively larger (green in Figure 7, bottom). The *intrinsic* energy transfer time scale from the antenna to the RC is 10 ps (Figure 6). In our model, however, RP1 forms a deep trap (1.5 ps) from which back transfer occurs to a much lesser extent (Figure 3) than in the model of Miloslavina (Figure 6). The *intrinsic* energy transfer time from the antenna to the RC is 20 ps (Figure 3), which is two times longer. Consequently, in our model, the direct antenna to RC energy transfer plays a more significant role in the *apparent* excited state decay time of the antenna than is the case in Miloslavina's model, which is ∼45 ps in both cases. The inverted kinetics mentioned earlier for the RC in the model of Figure 3 (Table 1) confirms this conclusion and suggests a non-negligible role for antenna to RC energy transfer in the total CS process.

From the X-ray structure of PSII cores, interpigment distances between CP43/CP47 and the RC appeared to be rather large with respect to the distances between the pigments in a single complex. This raised the question whether energy equilibration between the antenna and the RC could occur as fast as proposed by the ERPE model (<3 ps). The model according to Miloslavina et al[28] in Figure 6, shows forward and backward rates of respectively 100 and 344 ns^{-1} between the antenna and the RC. From our proposed model in Figure 3 we observe both rates to be smaller, that is, 50 and 200 ns^{-1} respectively. Consequently, the *intrinsic* energy equilibration time between the antenna and the RC will be larger in our modeling (Figure 3) than is the case in Miloslavina's model (Figure 6). Moreover, within our proposed model we were able to resolve the spectral evolution between the blue and "red" antenna pigment pools of CP43/CP47 (bA and A), with an *apparent* equilibration time of 7.5 ps. Referring to the X-ray structure, the equilibration between the CP43/CP47 antenna and the RC will take place on a much larger time scale than equilibration within the CP43/CP47 antenna. Furthermore, the *intrinsic* equilibration time between antenna and RC is about 4 ps from Figure 3. Both equilibration times within the antenna and between the antenna and the RC are thus larger than the proposed <3 ps equilibration time by the ERPE model. However, from Table 2 it is observed that Miloslavina's model results in an *apparent* energy equilibration time between antenna and RC of only 1.8 ps. Consequently, the model in Figure 3 is favored with respect to that proposed by Miloslavina et al,[28] because it is more consistent with the predictions from the X-ray structure.[15,22,23,25,40] Mutagenesis studies that perturb the radical pair free energy in a controlled way[41] could be useful to distinguish between both models.

The spectral degeneracy of the CP43 and CP47 antenna units with the RC causes time-resolved visible absorption and emission spectroscopy to be incapable to distinguish between the pigments of either complex. To this end, time-resolved infrared spectroscopy is required, since each complex has a specific infrared fingerprint. More importantly, Chl and Pheo have unique signatures in their different excited and charged states.[11] Thus, infrared spectroscopy could reveal the role of CS in the recorded slow decay phases. However, this type of experiment is not possible with low excitation light intensities, which are required to keep the RCs of PSII core open. Time-resolved infrared measurements have been performed on isolated RCs[11] and revealed the identity of the primary electron donor−acceptor pair ($Chl_{D1}^{+}Pheo^{-}$) as well as the ultrafast time scale on which it is formed, 0.6−0.8 ps. This ultrafast time scale of primary CS is in support of our modeling of the PSII core kinetics according to Figure 3, which resulted in 1.5 ps for RP1 formation over that proposed by Miloslavina et al.,[28] where 7.5 ps was found (Figure 6). Pawlowicz et al.[27] have measured the mid-infrared kinetics of PSII cores at room temperature. The data could be well fitted using the same kinetic model for the PSII core RC as was found for the isolated RC[11] and adding two slowly transferring antennae. From the target analysis, fast CS is found to occur in the PSII core on a time scale of 3 ps. The charge separated state is identified as $P_{D1}^{+}Pheo^{-}$. The $Chl_{D1}^{+}Pheo^{-}$ state is not observed and therefore concluded to have a very minor population. Consequently, $Chl_{D1}^{+}Pheo^{-}$ is assumed to be mixed with the excited RC in the applied model. $P_{D1}^{+}Pheo^{-}$ formation is determined to occur on a second time scale of 27 ps as well. The slow $P_{D1}^{+}Pheo^{-}$ formation is clearly shown to be due to the slow energy equilibration between the CP43/CP47 antenna and the RC, with 40 ps *intrinsic* energy transfer time constant from the antenna to the RC.[27] Note how the results presented in our paper (Figure 3, Table 1) agree with the biphasic RP1 formation and the slow energy transfer from the antenna to the RC found in the mid-infrared study of PSII cores. In contrast, Miloslavina et al.[28] assigned the 42 ps lifetime to slow radical pair formation. In fact, however, most of the antenna and RC also decay with this time constant (Table 2).

Finally, note that the free energy difference associated with RP1 formation in the model of Figure 3 is −110 meV, or 890 cm^{-1}, which is in full agreement with the simulations of ref 22, modeling two RPs, from which it was concluded that primary CS in open RCs of PSII membranes must be fast and nearly irreversible.

Time-Resolved Emission (77 K). To support the conclusions drawn from the room temperature measurements, that is, to show that the energy transfer from the antenna to the RC is slow, time-resolved emission was recorded of PSII cores at 77 K. Note

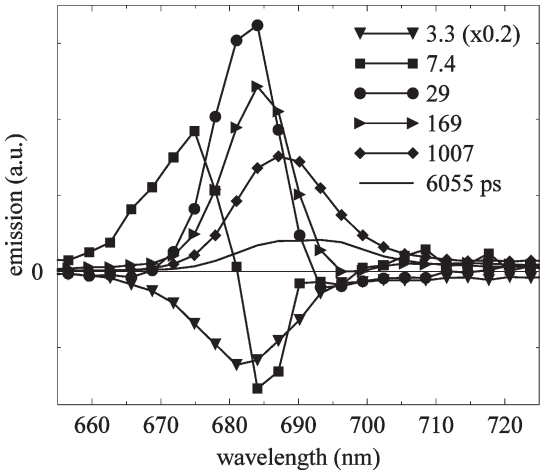

Figure 8. DAS of intact PSII cores at 77 K upon 400 nm excitation.

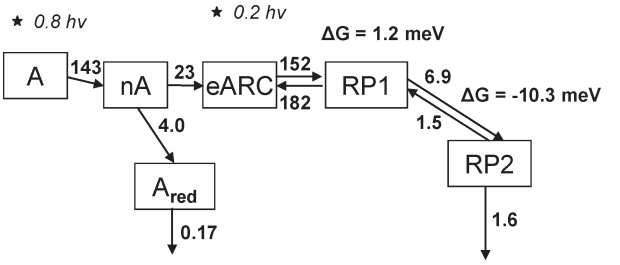

Figure 9. Kinetic model to describe the results of Figure 8. The compartment A represents all Chls in the CP43/CP47 antenna, which relax to the nonequilibrated bulk Chls of the antenna (nA). The compartment (eARC) represents the equilibrium between core antenna and excited RC. Two RPs (RP1, RP2) are in equilibrium with the RC and its associated core antenna. ★ indicates the initial excitation fractions: 80% A and 20% eARC. Rate constants (ns^{-1}) estimated are indicated in the figure as well as the free energies. Resulting lifetimes: 0.5, 3.3, 7, 37, 193, 1046, and 5000 ps. The estimated error in the lifetimes is 10%.

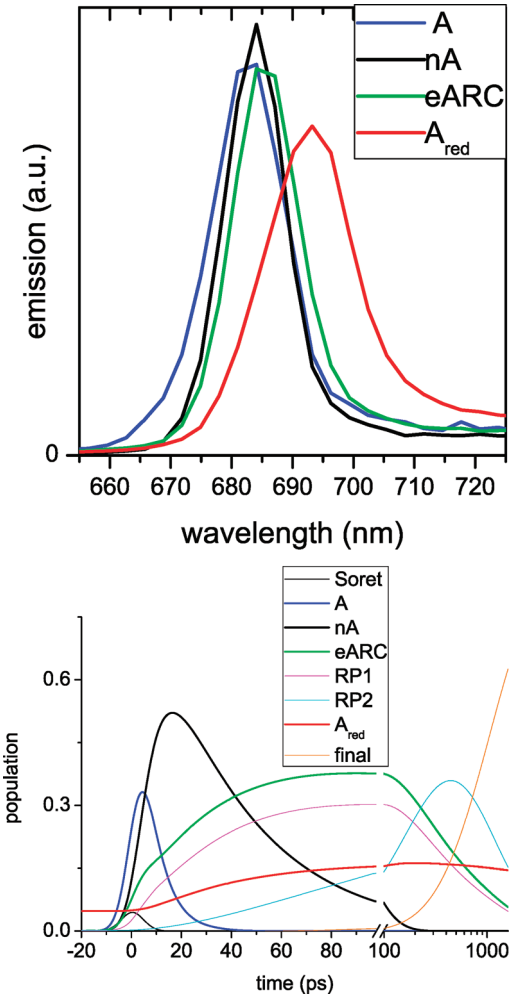

Figure 10. (Top) Estimated SAS from the model given in Figure 9. RPs are nonfluorescent. (Bottom) Population profiles of all species. Note that A_{red} is populated "before time zero" because of the backsweep of the synchroscan streak camera system.[31].

that, at this temperature and given the experimental conditions, it was not possible to keep the RCs open, but this is of no influence in estimating the excitation energy migration time. Although cryogenic temperatures promote selective excitation, to avoid artifacts introduced by the large contribution of Rayleigh scattering in this type of experiment, the time-resolved emission of PSII cores was recorded at 77 K upon 400 nm excitation.

The estimated DAS from global analysis are shown in Figure 8. Representative traces are depicted in Figure SI.2. An overall negative spectrum with maximum at 682 nm and a lifetime of 3.3 ps describes the Soret relaxation (note that the fwhm of the overall time response is 10 ps). At the 7.4 ps time scale energy transfer is clearly observed to occur from pigments emitting at 675 nm (positive amplitude) to those with emission wavelength at 685.5 nm (negative amplitude). Note that, because a significant rise of fluorescence is recorded (negative amplitude), CS in the RC can thus not be the main process occurring at this time scale. The main decay component has a lifetime of 29 ps, and its emission maximum is at 682.5 nm. At the same time scale, the small negative amplitude at long wavelengths indicates that a small amount of energy is transferred to pigments with emission maximum at 693 nm. A Chl *a* with this red emission wavelength is known to be located in CP47.[36,42,43] As a result, the 29 ps time constant will include the migration time of excitations in the CP47 antenna to the 693 nm trap. A decay phase with a time constant of 169 ps is observed with maximum emission at 684 nm (Figure 8). In an earlier study,[44] the main trapping phase in PSII membranes (BBY) and in intact photosynthetic membranes at 77 K was shown to have a similar lifetime of 150 ps. In BBY this spectrum is somewhat broader and the emission maximum is 3 nm blue-shifted,[44] due to the presence of light-harvesting complex II in the PSII supercomplex, which causes the excitation distribution to be blue-shifted. On the ns time scale, two more fluorescence decay phases are resolved with respective lifetimes of 1 and 6 ns (Figure 8 and Figure SI.2). The 1 ns decay component has an emission maximum at 688 nm, whereas the 6 ns component displays two peaks respectively at 687 and 695 nm, recognized as the PSII core steady-state emission spectrum at 77 K.[37] In BBY,[44] a phase with 500 ps decay time resembles the 1 ns phase resolved in cores (Figure 8). In the following, we will argue that this phase corresponds to the formation of a third radical pair. Therefore, the difference in this lifetime between cores and BBY will be due to the role of the antenna in determining the RP relaxation mechanism. Similarly, in BBY,[44] a phase with 4 ns lifetime and emission maximum at 693 nm was determined to represent trapping on the red pigments of CP47. In the core (Figure 8), the 6 ns

dx.doi.org/10.1021/jp1083746 |J. Phys. Chem. A XXXX, XXX, 000–000

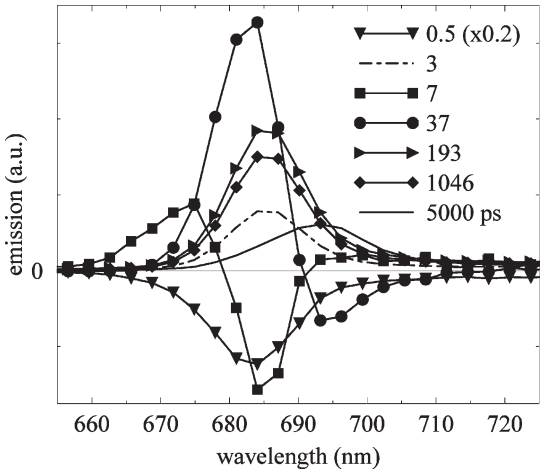

Figure 11. DAS calculated with the help of the kinetic model of Figure 9. See Table 3 for the associated amplitude matrix of the different compartments used in the model.

Table 3. Amplitude Matrix for the Target Analysis of the Time-Resolved Fluorescence of Intact PSII Cores at 77 K, as Represented in Figures 8−11[a]

	A	nA	eARC	RP1	RP2	A_{red}
τ (ps)	0.8 hν		0.2 hν			
3.0			0.130	−0.133	0.003	
7.0	0.8	−1.0	0.042	0.138	−0.007	0.030
37		1.0	−0.517	−0.461	0.135	−0.149
193			0.300	0.249	−0.798	
1046			0.245	0.207	0.667	
6024						0.119

[a] Negative amplitude represents a population rise, whereas positive amplitude shows population decay of the respective compartment with the specified lifetime.

spectrum has a clear contribution at 687 nm as well. We attribute this to the presence of a small fraction of free CP43/CP47 antenna units due to the freezing and thawing of the PSII core sample.

Kinetic Modeling. A target analysis was performed to identify the individual processes contributing to the DAS of Figure 8. The minimal model comprises six compartments, see Figure 9, which includes the optimal rate constants and the RP free energies. The compartments, respectively, represent bulk antenna (A), nonequilibrated antenna (nA), equilibrated antenna, and RC (eARC), RP1, RP2, and red pigments of CP47 (A_{red}). The eARC compartment consists of the RC in equilibrium with the CP43/CP47 antenna, because the S/N ratio of the data precluded the estimation of more equilibria than the ones shown in Figure 9, which are necessary to describe the charge-recombination. Similarly, the bulk (A) to nonequilibrated antenna (nA) energy transfer depicted in Figure 9 represents the blue to red Chl *a* energy relaxation taking place in the CP43 and CP47 antenna. The initial excitation population was chosen to be 80:0:20 between bulk antenna (A), nonequilibrated antenna (nA), and the antenna in equilibrium with the RC (eARC), thus, considering the blue to red Chl *a* energy relaxation in the CP43/CP47 antenna irreversible. This assumption is reasonable, because back transfer to blue antenna pigments will be significantly smaller at this temperature than at room temperature (Figure 3). Notice that we use a somewhat different approach to describe the 77 K data than those collected at room temperature (Figure 3). At 77 K the spectral resolution is much better due to the strong reduction of homogeneous broadening, though the S/N of the data is still insufficient to spectrally distinguish between CP43 and CP47. But we do, however, distinguish between internal antenna diffusion (A → nA) and transfer to the trap (nA → eARC), which is the purpose of this experiment. The 77 K SAS estimated from the modeling in Figure 9 are displayed in Figure 10 (top) and show overlap between bulk (A) and nonequilibrated antenna (nA), where the bulk antenna has extra emission amplitude at blue wavelengths due to which it has an emission maximum at 683 nm and the nonequilibrated antenna at 684 nm. The antenna in equilibrium with the RC (eARC) shows its emission maximum at 685.5 nm. The red pigments of CP47 show an emission maximum at 693 nm. RP1 and RP2 are nonfluorescent. The calculated DAS and amplitude matrix of the model in Figure 9 are respectively shown in Figure 11 and Table 3. The fluorescence rise as a result of Soret to Q_Y relaxation is fixed to take place on the subpicosecond time scale. The 3.3 ps lifetime DAS shows overall positive amplitude (Figure 11) with emission maximum at 685.5 nm. Primary CS is seen to dominate the 3.3 ps lifetime (Table 3), which is thus a factor two slower than for PSII cores with open RCs at room temperature (Table 1). This result is in good accordance with the estimated 1−4 ps time scale of RP1 formation in the isolated RC at 77 K.[45−47] On the 7 ps time scale, energy transfer is obviously taking place from Chls with emission maximum at 674 nm to those with emission at 685 nm (Figure 11). From the amplitude matrix (Table 3), the transfer is concluded to be due to blue to red Chl *a* excitation energy relaxation (A → nA) in the antenna, see also Figure 8. The lifetime and interpretation of this phase is almost identical to that of the corresponding phase with similar kinetics at room temperature. The 37 ps lifetime has a main positive contribution from nonequilibrated antenna (Table 3) and negative amplitude by RP1. Thus, RP1 formation is biphasic, with time scales of 3.3 and 37 ps, the latter being due to slow transfer from the antenna. This result is similar to that at room temperature, where direct CS from the RC occurs on the 1.5 ps time scale and slow transfer from the antenna resulted in a second formation time of 44 ps (Table 1). From the negative amplitude in Table 3, as well as that at 693 nm in Figure 11, it is concluded that also the red pigments of CP47 become populated at the time scale of 37 ps. Note how this *apparent* migration time scale in the CP47 antenna (37 ps) resembles that in the trimeric LHCII complex, which was estimated to be ∼32 ps,[48] and how this time scale is slower than measured before in isolated CP47 at 77 K.[38] From Table 3, both (RC) and (RP1) populations are observed to decay, whereas RP2 is seen to be formed on the 193 ps time scale. RP2 trapping is observed to give rise to the dominant fluorescence decay component (Figures 8, 10 (bottom), and 11), which is expressed by the −10 meV RP1-RP2 free energy difference with respect to the shallow RC-RP1 trap (1.2 meV; Figure 9). The 1 ns lifetime displays positive amplitudes from RC, RP1, and dominantly RP2 (Table 3), because it is the decay time of RP2 into the final RP trap state. Then, the excitations which were trapped on the red pigments of CP47 are seen to decay on the 6 ns time scale (Figure 11, Table 3), which agrees well with the 5.8 ns fluorescence lifetime of CP47 at 77 K.[38]

At 77 K, the CS in the PSII core will be different from that at room temperature, because Q_A is in its reduced form at this temperature. RP1, formed on the 3.3 ps time scale, is assigned to $Chl_{D1}^{+}Pheo^{-}$.[11] Electron transfer from RP1 to RP2 occurs on

dx.doi.org/10.1021/jp1083746 |J. Phys. Chem. A XXXX, XXX, 000–000

the time scale of 193 ps and RP2 is assigned to $P_{D1}^{+}Pheo^{-}$. The final RP trap in PSII cores with Q_A reduced is likely a relaxed state of $P_{D1}^{+}Pheo^{-}$.[47] Note that RP1 is nearly iso-energetic with the excited RC (1.2 meV; Figure 9) and, thus, forms an extremely shallow trap, causing the excitations to travel back and forth between the antenna, RC, and RP1 many times before trapping occurs. Consequently, the (RC) compartment, representing the RC in equilibrium with the CP43/CP47 antenna, shows large decay amplitudes at long time scales of 193 ps and 1 ns in the amplitude matrix of Table 3. The same is true for the decay amplitudes of RP1 (Table 3). At 77 K, the excited state decay in the closed PSII core will thus be trap-limited. From Table 3, the *apparent* energy transfer from the CP43/CP47 antenna into the RC is observed to take place on the time scale of 37 ps at 77 K. This agrees with a study of the effect of increasing the antenna size on RC dynamics with Q_A in its reduced form.[41] They concluded that the dynamics of charge separation are trap limited with closed RC.

Concluding, the 77 K experiment shows that excitation energy relaxation within the CP43 or CP47 antenna takes place at a time scale of 7 ps, which is similar to the value found at room temperature (7.7 ps). The excitation energy transfer from CP43 or CP47 to the RC was determined to occur on a 37 ps time scale at 77 K (Figure 9, Table 3), similar to the value found at room temperature (44 ps, Figure 3, Table 1). Note from Figure 9 that the excited state of the nonequilibrated antenna (A) does not become populated through back transfer from the RPs and as such represents the true energy transfer time among the antenna and RC. It is concluded that energy transfer from the antenna into the RC is slow in PSII cores. RP1 formation from the excited RC, however, occurs on a faster time scale at room temperature (1.5 ps) than at 77 K (3.3 ps). The latter is explained by the different RP relaxation mechanisms in the presence of oxidized Q_A at room temperature and reduced Q_A at 77 K.[37,47]

CONCLUSIONS

We have performed time-resolved fluorescence measurements of PSII cores with open, functional RCs at room temperature. By kinetic modeling, charge separation was found to occur on an ultrafast time scale of 1.5 ps, consistent with estimated ultrafast RP1 formation by femtosecond infrared spectroscopy.[11] RP1 formation was found to be virtually irreversible in this study, which is in accordance with modeling performed on time-resolved fluorescence data of PSII membranes with open RCs.[22] Energy equilibration within the antenna was found to take place at a time scale of 7.7 ps. Energy equilibration between the antenna and the RC was estimated to take place at a 44 ps time scale (Table 1). Slow energy transfer from the antenna to the RC, occurring with an estimated *intrinsic* time scale of 20 ps (Figure 3), plays a significant role in this equilibration time. Excitation energy equilibration between antenna and RC is thus found to occur on a larger time scale than proposed by the ERPE model (<3 ps) and consequently meets predictions from the X-ray structure.[15,22,23,25,40]

At 77 K, time-resolved fluorescence measurements of PSII cores revealed the energy equilibration time in the core antenna to be of similar size (7 ps), as was estimated at room temperature. The same is true for the excited state decay of the antenna, which was determined to occur at the time scale of 37 ps at 77 K. We conclude that population of the RC from the CP43/CP47 antenna takes place at a much longer time scale (>10×) than primary CS, both at room temperature and at 77 K. Consequently, the time scale of energy transfer from the CP43/CP47 antenna into the RC plays a significant role in the total CS kinetics in intact cores, due to which CS will not be purely trap-limited.

ASSOCIATED CONTENT

Supporting Information. Additional supporting data. This material is available free of charge via the Internet at http://pubs.acs.org.

ACKNOWLEDGMENT

We thank Eberhard Schlodder (Technische Universität Berlin) for kindly providing the samples and for useful discussions. Marloes Groot is thanked for critical reading of the text. This research is supported by The Netherlands Organization of Scientific Research (NWO) via the foundation of Earth and Life Sciences (ALW) and the Foundation for Fundamental Research on Matter (FOM).

REFERENCES

(1) van Grondelle, R.; Dekker, J. P.; Gillbro, T.; Sundström, V. *Biochim. Biophys. Acta* **1994**, *1187*, 1.
(2) Zouni, A.; Witt, H. T.; Kern, J.; Fromme, P.; Krauss, N.; Saenger, W.; Orth, P. *Nature* **2001**, *409*, 739.
(3) Ferreira, K. N.; Iverson, T. M.; Maghlaoui, K.; Barber, J.; Iwata, S. *Science* **2004**, *303*, 1831.
(4) Loll, B.; Kern, J.; Saenger, W.; Zouni, A.; Biesiadka, J. *Nature* **2005**, *438*, 1040.
(5) Guskov, A.; Kern, J.; Gabdulkhakov, A.; Broser, M.; Zouni, A.; Saenger, W. *Nat. Struct. Mol. Biol.* **2009**, *16*, 334.
(6) Dekker, J. P.; Boekema, E. J. *Biochim. Biophys. Acta, Bioenerg.* **2005**, *1706*, 12.
(7) Diner, B. A.; Rappaport, F. *Annu. Rev. Plant Biol.* **2002**, *53*, 551.
(8) Novoderezhkin, V. I.; Dekker, J. P.; van Grondelle, R. *Biophys. J.* **2007**, *93*, 1293.
(9) Romero, E.; van Stokkum, I. H. M.; Novoderezhkin, V. I.; Dekker, J. P.; van Grondelle, R. *Biochemistry* **2010**, *49*, 4300.
(10) Van Brederode, M. E.; Jones, M. R.; Van Mourik, F.; Van Stokkum, I. H. M.; Van Grondelle, R. *Biochemistry* **1997**, *36*, 6855.
(11) Groot, M. L.; Pawlowicz, N. P.; van Wilderen, L.; Breton, J.; van Stokkum, I. H. M.; van Grondelle, R. *Proc. Natl. Acad. Sci. U.S.A.* **2005**, *102*, 13087.
(12) Holzwarth, A. R.; Muller, M. G.; Reus, M.; Nowaczyk, M.; Sander, J.; Rogner, M. *Proc. Natl. Acad. Sci. U.S.A.* **2006**, *103*, 6895.
(13) Barter, L. M. C.; Durrant, J. R.; Klug, D. R. *Proc. Natl. Acad. Sci. U.S.A.* **2003**, *100*, 946.
(14) Dekker, J. P.; Van Grondelle, R. *Photosynth. Res.* **2000**, *63*, 195.
(15) Renger, T.; Schlodder, E. *ChemPhysChem* **2010**, *11*, 1141.
(16) Schatz, G. H.; Brock, H.; Holzwarth, A. R. *Proc. Natl. Acad. Sci. U.S.A.* **1987**, *84*, 8414.
(17) Renger, G.; Eckert, H. J.; Bergmann, A.; Bernarding, J.; Liu, B.; Napiwotzki, A.; Reifarth, F.; Eichler, H. J. *Aust. J. Plant Physiol.* **1995**, *22*, 167.
(18) Hodges, M.; Moya, I. *Biochim. Biophys. Acta* **1988**, *935*, 41.
(19) Schatz, G. H.; Brock, H.; Holzwarth, A. R. *Biophys. J.* **1988**, *54*, 397.
(20) van Grondelle, R. *Biochim. Biophys. Acta* **1985**, *811*, 147.
(21) Van Mieghem, F. J. E.; Searle, G. F. W.; Rutherford, A. W.; Schaafsma, T. J. *Biochim. Biophys. Acta* **1992**, *1100*, 198.
(22) Broess, K.; Trinkunas, G.; van der Weij-de Wit, C. D.; Dekker, J. P.; van Hoek, A.; van Amerongen, H. *Biophys. J.* **2006**, *91*, 3776.
(23) Vasil'ev, S.; Orth, P.; Zouni, A.; Owens, T. G.; Bruce, D. *Proc. Natl. Acad. Sci. U.S.A.* **2001**, *98*, 8602.
(24) Vassiliev, S.; Lee, C. I.; Brudvig, G. W.; Bruce, D. *Biochemistry* **2002**, *41*, 12236.
(25) Raszewski, G.; Renger, T. *J. Am. Chem. Soc.* **2008**, *130*, 4431.
(26) Vassiliev, S.; Bruce, D. *Photosynth. Res.* **2008**, *97*, 75.

(27) Pawlowicz, N. P.; Groot, M. L.; van Stokkum, I. H. M.; Breton, J.; van Grondelle, R. *Biophys. J.* **2007**, *93*, 2732.
(28) Miloslavina, Y.; Szczepaniak, M.; Muller, M. G.; Sander, J.; Nowaczyk, M.; Rogner, M.; Holzwarth, A. R. *Biochemistry* **2006**, *45*, 2436.
(29) Broess, K.; Trinkunas, G.; van Hoek, A.; Croce, R.; van Amerongen, H. *Biochim. Biophys. Acta, Bioenerg.* **2008**, *1777*, 404.
(30) Fleming, G. R.; Morris, J. M.; Robinson, G. W. *Aust. J. Chem.* **1977**, *30*, 2337.
(31) van Stokkum, I. H. M.; van Oort, B.; van Mourik, F.; Gobets, B.; van Amerongen, H. (Sub)-Picosecond Spectral Evolution of Fluorescence Studied with a Synchroscan Streak-Camera System and Target Analysis. In *Biophysical Techniques in Photosynthesis*; Aartsma, T. J., Matysik, J., Eds.; Springer: Dordrecht, The Netherlands, 2008; Vol. II, p 223.
(32) Komura, M.; Itoh, S. *Photosynth. Res.* **2009**, *101*, 119.
(33) Kern, J.; Loll, B.; Luneberg, C.; DiFiore, D.; Biesiadka, J.; Irrgang, K. D.; Zouni, A. *Biochim. Biophys. Acta, Bioenerg.* **2005**, *1706*, 147.
(34) Holzwarth, A. R. Data Analysis of Time-Resolved Measurements. In *Biophysical Techniques in Photosynthesis*; Amesz, J., Hoff, A. J., Eds.; Kluwer: Dordrecht, The Netherlands, 1996; p 75.
(35) van Stokkum, I. H. M.; Larsen, D. S.; van Grondelle, R. *Biochim. Biophys. Acta, Bioenerg.* **2004**, *1657*, 82.
(36) de Weerd, F. L.; Palacios, M. A.; Andrizhiyevskaya, E. G.; Dekker, J. P.; van Grondelle, R. *Biochemistry* **2002**, *41*, 15224.
(37) Andrizhiyevskaya, E. G.; Chojnicka, A.; Bautista, J. A.; Diner, B. A.; van Grondelle, R.; Dekker, J. P. *Photosynth. Res.* **2005**, *84*, 173.
(38) de Weerd, F. L.; van Stokkum, I. H. M.; van Amerongen, H.; Dekker, J. P.; van Grondelle, R. *Biophys. J.* **2002**, *82*, 1586.
(39) van Mourik, F.; Groot, M. L.; van Grondelle, R.; Dekker, J. P.; van Stokkum, I. H. M. *Phys. Chem. Chem. Phys.* **2004**, *6*, 4820.
(40) Saito, K.; Kikuchi, T.; Nakayama, M.; Mukai, K.; Sumi, H. *J. Photochem. Photobiol., A* **2006**, *178*, 271.
(41) Barter, L. M. C.; Bianchietti, M.; Jeans, C.; Schilstra, M. J.; Hankamer, B.; Diner, B. A.; Barber, J.; Durrant, J. R.; Klug, D. R. *Biochemistry* **2001**, *40*, 4026.
(42) den Hartog, F. T. H.; Dekker, J. P.; van Grondelle, R.; Volker, S. *J. Phys. Chem. B* **1998**, *102*, 11007.
(43) Groot, M. L.; Breton, J.; van Wilderen, L.; Dekker, J. P.; van Grondelle, R. *J. Phys. Chem. B* **2004**, *108*, 8001.
(44) van der Weij-de Wit, C. D.; Ihalainen, J. A.; van Grondelle, R.; Dekker, J. P. *Photosynth. Res.* **2007**, *93*, 173.
(45) Visser, H. M.; Groot, M. L.; Van Mourik, F.; Van Stokkum, I. H. M.; Dekker, J. P.; Van Grondelle, R. *J. Phys. Chem.* **1995**, *99*, 15304.
(46) Groot, M. L.; van Mourik, F.; Eijckelhoff, C.; van Stokkum, I. H. M.; Dekker, J. P.; van Grondelle, R. *Proc. Natl. Acad. Sci. U.S.A.* **1997**, *94*, 4389.
(47) Konermann, L.; Gatzen, G.; Holzwarth, A. R. *J. Phys. Chem. B* **1997**, *101*, 2933.
(48) Barzda, V.; Gulbinas, V.; Kananavicius, R.; Cervinskas, V.; van Amerongen, H.; van Grondelle, R.; Valkunas, L. *Biophys. J.* **2001**, *80*, 2409.